RSC Advances




ROYAL SOCIETY OF CHEMISTRY

www.rsc.org/advances

# Structural transition of $VO_2$ (A) nanorods studied by vibrational spectroscopies

**Jiwei Hou,[a] Jianwu Zhang,*[a] Zhongping Wang,[b] Zengming Zhang,[b] and Zejun Ding[a]**

[a] *Department of Physics and Hefei National Laboratory for Physical Sciences at Microscale, University of Science and Technology of China, Hefei, Anhui 230026, China. Fax: +86-551-63600614; Tel: +86-551-63600614; E-mail: zjw@ustc.edu.cn*
[b]*The centre of Physical Experiments, University of Science and Technology of China, Hefei, Anhui 230026, China.*

## Graphical Abstract

The temperature-induce phase transition of $VO_2$ (A) nanorods was observed from the Raman spectrum

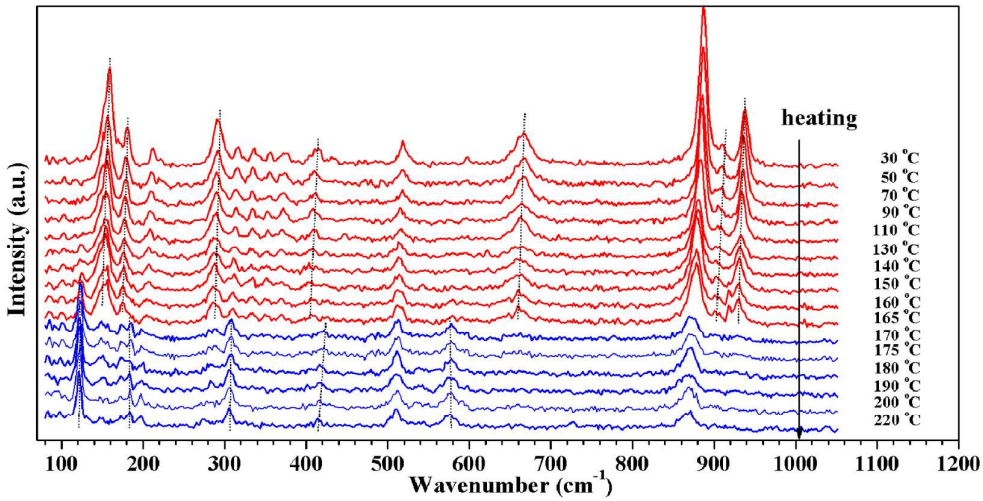


Temperature-dependent Raman spectra of the $VO_2$ (A) during the increasing temperature

Cite this: DOI: 10.1039/c0xx00000x

www.rsc.org/xxxxxx

ARTICLE TYPE

# Structural transition of $VO_2$ (A) nanorods studied by vibrational spectroscopies

**Jiwei Hou,[a] JianwuZhang,*[a] Zhongping Wang,[b] Zengming Zhang,[b] and Zejun Ding[a]**

*Received (in XXX, XXX) XthXXXXXXXXX 20XX, Accepted Xth XXXXXXXXX 20XX*

**DOI: 10.1039/b000000x**

**Single crystalline metastable phase $VO_2$ (A) nanorods were successfully synthesized by using a hydrothermal method, and the evolution of vibrational modes of $VO_2$ (A) nanorods have been observed in the vicinity of the structural phase transition. Fourier transform infrared (FT-IR) spectroscopy was employed to study the structural phase transition, and the abrupt changes of vibratory absorption bands at different temperatures showed a reversible phase transition. Raman spectrum measurement was performed to observe firstly the temperature-induced phase transition of $VO_2$ (A) nanorods. The Raman modes near the phase transition temperature display the phonon soften behaviour.**

## Introduction

In recent years many low-dimensional nanomaterials, such as nanowires, nanorods, nanobelts and nanotubes, have become the focus of great interest due to their fundamental research importance and wide range of unique application in fabrication of nanoscale devices,[1-3] which exhibit novel physical and chemical properties comparing with those of bulk materials. Vanadium dioxide ($VO_2$) nanostructures have attracted increasing attention because of many promising properties for various potential applications in the nanometer regime.[4-7] Vanadium dioxide is a representative binary compound having different polymorphs, including $VO_2$ (M), $VO_2$ (R), $VO_2$ (B) and $VO_2$ (A) and recently reported $VO_2$ (C).[8-9] Among these polymorphs, the rutile phase $VO_2$ (R) is the most thermodynamic stable phase and has been attracting much attention for the reason that it has been observed a reversible metal-insulator phase transition, from a low temperature monoclinic phase $VO_2$ (M) to a high temperature rutile phase $VO_2$ (R), at around 68 ºC.[10] Accompanied with this phase transition, $VO_2$ (R) shows a reversible abrupt changes in the electrical, magnetic and optical properties, especially for optical properties in the infrared region.[11] Such properties make $VO_2$ (R) potential applications in many fields, such as the gas sensor, optical switching devices, Mott field-effect transistors and the optical data storage media.[12-14] Meanwhile, the structures, properties and potential applications of metastable $VO_2$ (B) as a high potential candidate for the cathode materials in lithium-ion batteries have been widely studied. In addition, $VO_2$ (B) as a precursor for preparing $VO_2$ (R) has also been widely studied. We have investigated previously the monoclinic $VO_2$ nanoparticles; the phase transition temperature was effectively controlled by the different W-doped concentrations.[15] However, another metastable phase $VO_2$ (A), which also exhibits a similar temperature-induced structural phase transition, has been paid less attention for the reason that this metastable phase is usually absent during the preparation of $VO_2$ polymorph.

The presence of metastable phase $VO_2$ (A) was firstly reported by Théobald via a hydrothermal reaction of the $V_2O_3$-$V_2O_5$-$H_2O$ system.[16] Several decades later, Oka et al have prepared $VO_2$ (A) by a hydrothermal method and studied the crystal structures of the low temperature and high temperature phases of $VO_2$ (A).[17] Subsequently, based on the crystal structure of $VO_2$ (A), thermal stability, optical properties and electrical properties of $VO_2$ (A) have been investigated.[18-19] The study on the physical properties of $VO_2$ (A) shows that $VO_2$ (A) undergoes a reversible structural phase transition from its low temperature tetragonal phase to the high temperature body-center tetragonal phase ($A_H$) at around 162 ºC. The high temperature X-ray analysis showed that the phase transition of $VO_2$ (A) is originated in the dissociation of the $V^{4+}$-$V^{4+}$ pairs along the *c*-axis.[20] Meanwhile, a simple crystallographic slip mechanism was proposed to explain the phase transition process from $VO_2$ (B) to $VO_2$ (A).[21] The Raman signal of $VO_2$ (A) is very weak and thermal heating sensitive; even several mW of fine focused laser radiation is enough to induce the phase transition in $VO_2$ (A). There were no reports on studying structural phase transition of $VO_2$ (A) nanostructures by using vibrational spectroscopy, including Raman and FT-IR spectroscopy. In this work, we have greatly reduced the incident light intensity to avoid phase transition due to thermal heating of fine focused laser beam. The vibrational spectra of $VO_2$ (A) were successfully observed during the phase transition.

To the best of our knowledge, vibrational spectroscopy had been used to study the structural phase transition of $VO_2$ (M/R).[22-23] In contrast to $VO_2$ (M/R), metastable phase $VO_2$ (A) has been comparatively attracted less attention, and there are no reports on the study of phase transition of $VO_2$ (A) nanostructures by using Raman and FT-IR spectroscopies. In the present study, we have developed a facile way to prepare single crystalline $VO_2$ (A) nanorods by a hydrothermal method; we report the investigation of the phase transition of $VO_2$ (A) nanorods by using Raman scattering and FT-IR spectroscopy spectra. The evolution of vibrational modes of $VO_2$ (A) nanorods is discussed for the temperatures near the phase transition.

## Experimental

The single crystalline metastable phase $VO_2$ (A) nanorods were synthesized by a hydrothermal method using $VOSO_4$ as the raw material. In a typical procedure, a given amount of $VOSO_4$ powder was dispersed into 80 ml of deionized water to form a clear blue solution after stirring for 30 minutes, and then the blue solution was transferred into a 100 ml Teflon-lined autoclave with a stainless steel shell at 220 ºC for 24 h. When the reaction was finished, the autoclave was cooled naturally down to room temperature. Then the resulting brown slurry was collected by centrifugation, washed with distilled water and ethanol for several times, and finally dried in vacuum at 60 ºC for 8 h.

The crystal structure of obtained samples was recorded on a Shimadzu X-ray diffraction-7000 with Cu-Kα radiation. Morphology of the sample was observed with a field emission scanning electron microscope (SEM, Hitachi S-4800). The transmission electron microscopy (TEM) images, high resolution transmission electron microscopy (HRTEM) images and selected area electron diffraction (SAED) patterns were acquired on a JEOL-2010 transmission electron microscope at an acceleration voltage of 200 kV. X-ray photoelectron spectroscopy (XPS) measurements were performed on a VGESCALAB MKII X-ray photoelectron spectrometer with an excitation source of Mg-Kα, 1253.6 eV. Differential scanning calorimetery (DSC) was measured by a NETZSCH DSC 200 from 20 to 200 ºC with the heating rate of 10 ºC $min^{-1}$. The FT-IR spectra of the samples, using pressed KBr tablets, were detected on a TENSOR-37 with an adapted heating controlled cell. The Raman spectra were recorded by using an integrated laser Raman system (LABRAMHR, Jobin Yvon) with a confocal microscope and a thermoelectrically cooled multichannel charge-coupled device (CCD) detection system; the spectral resolution was better than 1 $cm^{-1}$. The line 514.5 nm of an argon laser was used as excitation source with a power less than 10 mW. All Raman spectra were measured in the backscattering geometry at the different temperatures.

## Results and Discussion

Fig. 1(b) presents a typical XRD pattern of the as-obtained product; all the diffraction peaks can be perfectly indexed to the metastable tetragonal crystalline phase of $VO_2$ (A) (space group: P42/ncm, a=8.434 Å, c=7.681 Å), in agreement with the literature values (JCPDS No. 80-0690, a=8.434 Å, c=7.678 Å), whose plots are shown in Fig. 1(a). No characteristic peaks of any other phases and impurities are detected, indicating the as-obtained product with high purity. It is noteworthy that the stronger peaks belongs to the (*hk*0) family, suggesting that the $VO_2$ (A) nanorods have a preferential growth direction along the [110], which is in agreement with HRTEM and SAED analysis (Fig. 3(d)).

The surface composition of as-obtained sample was analyzed with XPS spectrum shown in Fig. 2. No peaks of elements other than C, O and V are observed on the survey spectrum. The peaks for O can be attributed to the $VO_2$, $O_2$, $CO_2$ or $H_2O$; the C1s peak is due to $CO_2$ absorbed on the sample surface. According to the literature, two peaks at 516.2 and 523.8 eV in the high resolution spectrum (inset of Fig. 2) are attributed to the spin-orbit splitting of $V_{2p3/2}$ and $V_{2p1/2}$ and the intensity ratio is near 2:1, which is the characteristic of vanadium in the +4 oxidation state.[24]

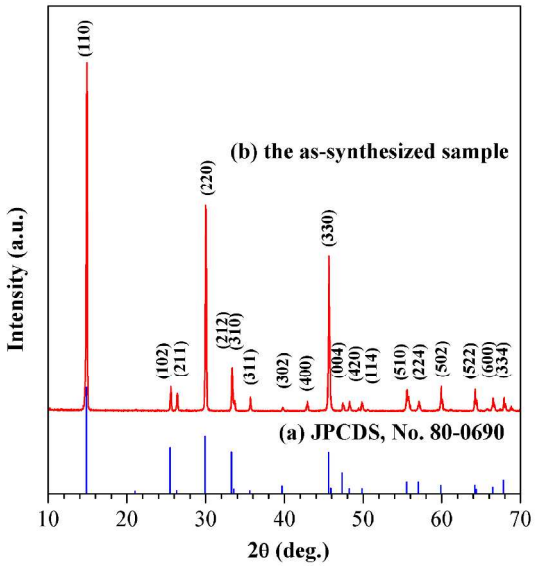


Fig. 1 X-ray diffraction patterns for (a) standard JPCDS; (b) as-synthesized $VO_2$ (A)

The other peaks at 631.0, 69.0 and 40.0 eV are attributed to V2s, $V_{3s}$ and $V_{3p}$ excitations, respectively. Consequently, the as-obtained sample can be determined as high pure tetragonal $VO_2$ (A) on basis of the results of XRD and XPS measurements.

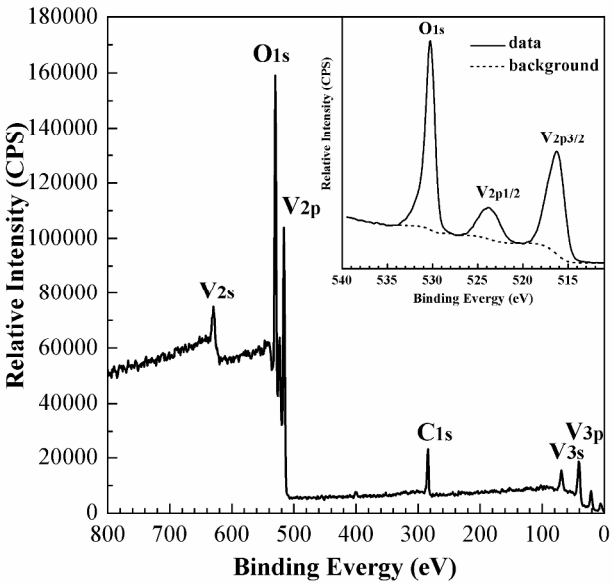


Fig. 2 The survey XPS spectrum of the $VO_2$ (A) (the inset is V2p peaks of $VO_2$ (A) nanorods)

The detailed morphology and microstructure of samples were investigated by SEM and TEM analysis; the typical SEM images of $VO_2$ (A) at different magnifications are shown in Fig. 3. $VO_2$ (A) nanorods with the rod-like morphology and in length of several tens of micrometers are clearly displayed. The average diameter of nanorods is about 200 nm in Fig. 3(b). The diameter statistics of $VO_2$ (A) nanorods have been given (Fig. S1, ESI†). A HRTEM image of a single nanorod and a SAED pattern (the

lower inset in Fig. 3(d)) obtained from the same single nanorod are shown in Figs. 3(c) and 3(d), respectively. The lattice fringes are clearly exhibited and the 0.536 nm of neighboring fringe spacing matches well the separation between (110) lattice planes. The corresponding SAED pattern further demonstrates that the nanorod is single crystalline and growth direction is along the [110] direction.

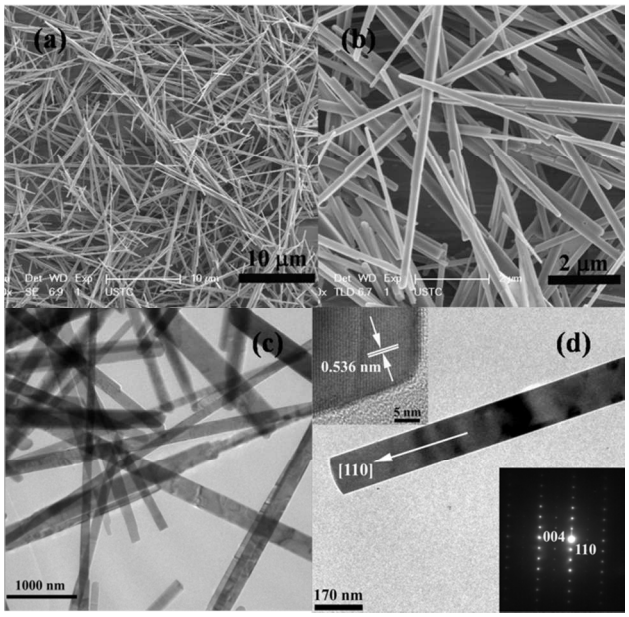


Fig. 3 Typical field emission SEM (a), high magnified SEM (b), low-resolution TEM (c) of $VO_2$ (A) nanorods, TEM image of a single nanorod (d) (insets are its corresponding SAED pattern and HRTEM image)

In order to further investigate the structure of $VO_2$ (A) nanorods *in situ* variable temperature X-ray diffraction measurements were performed on a Pt substrate in the temperature range from 25 to 220 ºC. The evolution of the XRD patterns of $VO_2$ (A) nanorods as a function of temperature is exhibited in Fig. 4.

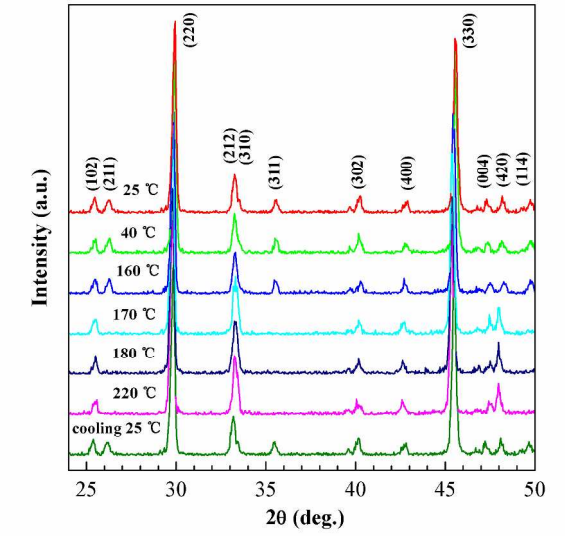


Fig. 4 Variable temperature XRD patterns of $VO_2$ (A) nanorods

The XRD pattern at lower temperature of 160 ºC can be readily indexed into low-temperature $VO_2$ (A) phase, while that above 170 ºC is assigned to a high-temperature phase $VO_2$ ($A_H$). The shape of the XRD pattern has almost no obvious change with temperature increasing except the disappearance of the (211), (310), (311), (420) and (114) diffraction peaks above phase transition temperature, indicating that the crystal structure does not change drastically. The disappearance of the diffraction peaks above the phase transition temperature, indicating that there are two different crystal structures of $VO_2$ (A) between 160 and 170 ºC. The XRD pattern at 25 ºC is reproduced upon cooling down from 220 ºC, the reversible change of the diffraction peaks confirms a reversible phase transition between initial phase and high temperature phase during heating and cooling processes.

The evolution of the lattice parameters associated with the temperature has been calculated and a slight increase of lattice parameter, *a*- and *b*-values, is observed from 8.434 Å to 8.472 Å (heat-treated at 220 ºC) and an obvious change of the lattice parameter *c*-value is observed from 7.684 Å to 3.821 Å (heat-treated 220 ºC). The results of lattice parameters are consistent with previously reported.[21] The *a/c* ratio in the tetragonal phase is increased from 1.098 to 2.216 with increasing temperature.

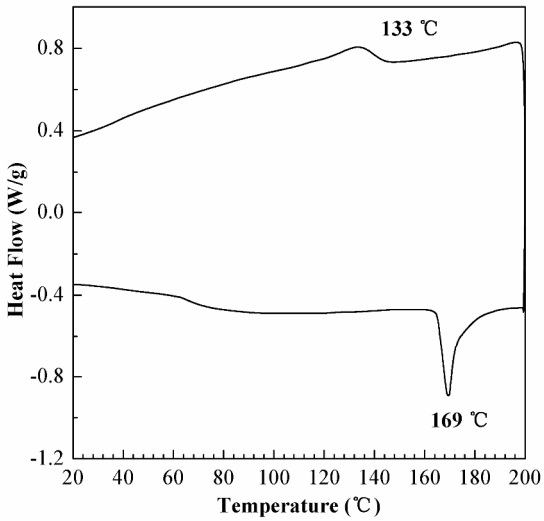


Fig. 5 DSC curve of $VO_2$ (A) nanorods under nitrogen at a heating rate of 10 ºC $min^{-1}$

Phase transition in $VO_2$ system using DSC analysis has been studied widely especially for monoclinic phase $VO_2$ (M/R), for which the first order metal-insulator phase transition occurs at 68 ºC.[25-26] In order to investigate the phase transition properties of $VO_2$nanorods, the DSC analysis was performed. There is an endothermic peak at 169 ºC and an exothermic peak at 133 ºC, as show in Fig. 5, in DCS curve. The DSC data show that the structure phase transition temperature of $VO_2$ (A) nanorods exist the obviously thermal hysteresis phenomenon. The endothermic peak at 169 ºC can be assigned to conversion of the initial tetragonal into a high-temperature phase during heating process. Meanwhile, an exothermic peak at 133 ºC can be attributed to the crystallization of the $VO_2$ ($A_H$) into the $VO_2$ (A) form upon cooling. The wide hysteresis loop of $VO_2$ (A) nanorods is considered to be due to the scaling to nanoscale domain, as observed in $VO_2$ (M/R) nanostructures.[27] The endothermic peak was slightly higher than162 ºC reported in the literatures due to the size effect and morphology of the nanostructure. Meanwhile,

effects of size and morphology of monoclinic $VO_2$ metal-insulator phase transition has been extensively studied.[28]

FT-IR spectroscopy is an excellent analytical method, which has been widely utilized to study the metal-insulator transition of $VO_2$ (M/R) nanostructures.[15,29] In order to observe the evolution behavior of vibrational modes of $VO_2$ (A) nanorods in the phase transition, an *in situ* variable-temperature IR spectroscopy was performed to further study the vibration bands. A series of FT-IR spectra of the as-obtained $VO_2$ (A) nanorods under varied temperatures are presented in Fig. 6. At 25 ºC, the IR spectra of single domain $VO_2$ (A) nanorods clearly display the existence of various V-O vibrations. According to the reported IR spectra of vanadium dioxide, the vibration band at 932 $cm^{-1}$ is assigned to the stretching of V=O bonds, while the bands at 548 and 426 $cm^{-1}$ are attributed to the long-rang stretching of V-O-V vibration modes. The bands at 980 $cm^{-1}$ or 1020 $cm^{-1}$ are absent, which are the characteristic peaks of $V^{3+}$ or $V^{5+}$,[26-27] respectively, which is consistent with our XRD results.

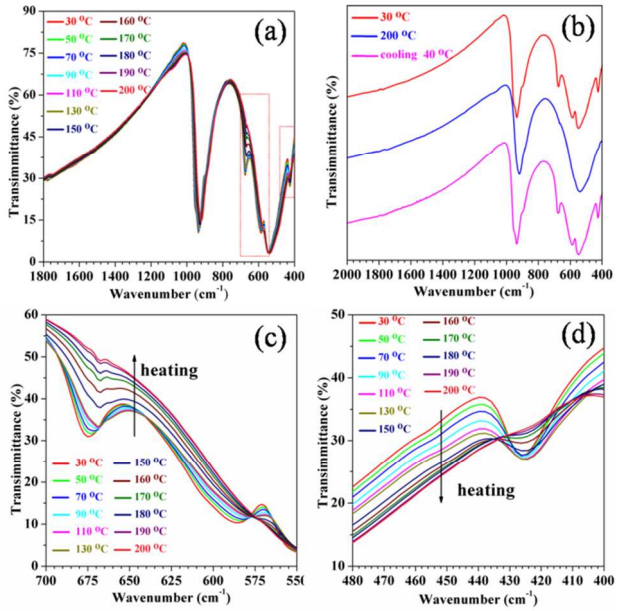


Fig. 6 Temperature-dependent IR spectra of the $VO_2$ (A)nanorods (a), IR spectra of $VO_2$ (A) nanorods at various temperatures (b), magnified spectra of the rectangular area in (a) at various temperatures (c),(d)

The temperature-dependent FT-IR spectra of the $VO_2$ (A) nanorods were investigated the phase transition. The IR spectra in Fig.6 display various V-O vibrations, and the vibration bands at 935 and 547 $cm^{-1}$ gradually shifted to lower wavenumbers with increasing temperature. The slight red shift of vibration bands indicates a phonon mode soften behavior. Figs. 6(c) and 6(d) show that the vibratory absorption bands at 670, 580 and 426 $cm^{-1}$ become gradually weaken and disappear with increasing temperature, while these bands reappear with lowering down temperature in Fig. 6(b).This optical property has a potential application in optical switching devices and the similar optical property was observed in $VO_2$ (M/R).[15,26,29] The FT-IR spectrum is usually interpreted as that the observed bands are related to the electromagnetic resonance between the incident photons and variation of chemical bond polarization associated with a specific vibration mode. The $V^{4+}$-$V^{4+}$ bonds in low temperature $VO_2$ (A) phase with a distance of 2.769 Å is dissociated in high temperature $VO_2$ (A) phase with a distance of 3.079 Å reported by Oka.[17] At low temperature the electrons involving in the $V^{4+}$-$V^{4+}$ bonds between $VO_6$ octahedraare localized, whereas these electrons are delocalized at high temperature. This delocalization involves a screening effect for the incident photons and leads to the vibration bands disappeared during increasing temperature.

In order to study the temperature induced phase transition of $VO_2$ (A) nanorods, an *in situ* Raman scattering measurement was performed under different temperatures. We reduced the incident laser intensity by about two orders to be roughly 0.1 mW to ensure that thermal heating due to focusing laser would not result in a phase transition. The evolution of Raman modes for $VO_2$ (A) nanorods under various temperatures is presented in Fig. 7 (a: heating, b: cooling). Ten Raman active modes are observed in the Raman spectrum for 30 ºC at 159, 180, 212, 291, 413, 518, 666, 887, 910 and 938 $cm^{-1}$, which are different with the known Raman modes of $VO_2$ (M/R).[32]

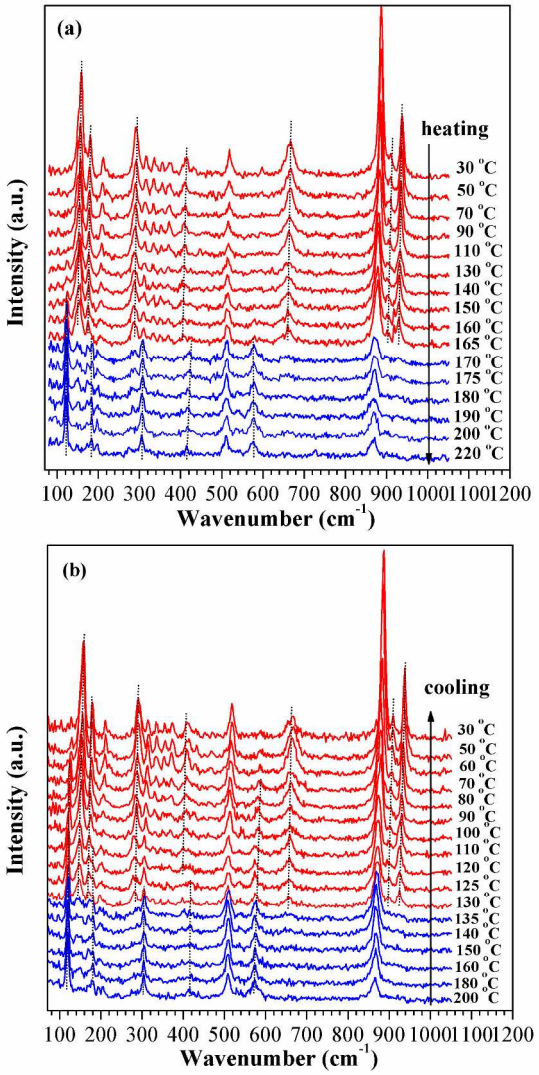


Fig. 7 Temperature-dependent Raman spectra of the $VO_2$ (A): (a) heating (b) cooling

For temperatures up to 165 ºC, all the Raman modes are assigned to the low temperature phase. At 170 ºC, some new Raman

modes appear at 123, 184, 308 422 and 578 $cm^{-1}$, which are the characteristic peaks of high temperature phase of $VO_2$ (A); the intensity of these new Raman modes become stronger and shaper with increasing temperature. Meanwhile, the Raman modes of the low temperature phase with frequencies at 159, 180, 291, 416, 666, 910 and 938 $cm^{-1}$ abruptly disappear. The discontinuities of Raman modes with temperature are clearly observed between 165 and 170 ºC, indicating a temperature-induced phase transition occurred between 165 and 170 ºC. The Raman vibrational modes of low temperature phase are fully restored during the temperature cooling down to ambient condition. The cooling process in the variable temperature Raman measurement show the reversible structure transition between 130 and 135 ºC in Fig. 7 (b). The results are well in agreement with the variable temperature X-ray diffraction and DSC data.

The evolution of the Raman modes appears to be almost linear until the temperature up to 165 ºC. The relationship between Raman peaks and temperature is fitted linearly with the slope called red shift coefficient α. The red shift coefficients determined from the fits are: α=0.059, 0.044, 0.052, 0.067, 0.074 and 0.089 $cm^{-1}$/K for 160, 180, 413, 887, 910 and 938$cm^{-1}$, respectively. It can be seen that the Raman modes exhibit an obvious red shift, indicating the electron interaction with the lattice is enhanced during the increasing the crystal temperature. An evidence of phonon softening behavior near the phase transition of $VO_2$ (A) was observed. The phonon soften behavior indicates that the driving mechanism of the phase transition of $VO_2$ (A) involve electron-phonon interaction. The electron-phonon interaction has been extensively studied using the Raman spectrum in the metal-insulator transition of $VO_2$ (M/R); the experimental and theoretical studies have confirmed that the electron-phonon interaction plays a crucial role in the metal-insulator transition of $VO_2$ (M/R).[33-34]

## Conclusions

In summary, $VO_2$ (A) nanorods were successfully fabricated through a facile and environmental friendly hydrothermal method without using any surfactants or templates. The as-obtained nanorods have diameters of 100-300 nm and length of several tens of micrometers. A reversible structural phase transition around 160-170 ºC has been observed through the variable-temperature X-ray diffraction and Raman spectroscopy measurement. An evidence of phonon softening behavior near the temperature of phase transition was observed through the variable-temperature vibrational spectrum. The electron-phonon interaction plays a role in the phase transition of $VO_2$ (A) nanorods.

## Acknowledgements

This work was supported by the National Natural Science Foundation of China (Grant Nos. 11174265, 11274288 and 21002097) and "973" projects (Nos. 2011CB932801, 2012CB933702 and 2009CB939901).

## Notes and references

[a]*Department of Physics and Hefei National Laboratory for Physical Sciences at Microscale, University of Science and Technology of China, Hefei, Anhui 230026, China. Fax: +86-551-63600614; Tel: +86-551-63600614; E-mail: zjw@ustc.edu.cn*
[b]*The centre of Physical Experiments, University of Science and Technology of China, Hefei, Anhui 230026, China.*

1 C.R. Xiong, A. E. Aliev, B. Gnade and K. J. Balkus, *ACS Nano.*, 2008, **2**, 294.
2 Z. Gui, R. Fan, W. Q. Mo, X. H. Chen, L. Yang and W. C. Fan, *Chem.Mater.*, 2002, **14**, 5055.
3 C. Nethravathi, B. Viswanath, J. Michael and M. Rajamath, *Carbon*, 2012, **50**, 4841.
4 C. H. Chen, R. F. Wang, L. Shang and C. F. Guo, *Appl. Phys. Lett.*, 2008, **93**, 171101.
5 J. M. Wu and L. B. Liou, *J. Mater. Chem.*, 2011, **21**, 5503.
6 X. H. Rui, D. H. Sim, C. Xu, W. L. Liu, H. T. Tan, K. M. Wong, H. H. Hng, T. M. Lim and Q. Y. Yan, *RSC Adv.*, 2012, **2**, 1178.
7 L. Dai, Y. F. Gao, C. X. Cao, Z. Chen, H. J. Luo, M. Kanehira, J. Jin and Y. Liu, *RSC Adv.*, 2012, **2**, 5268.
8 C. Leroux, G. Nihoul and G. V. Tendeloo, *Phys. Rev. B*, 1998, 57, 5111.
9 D. Hangrman, J. Zubieta, C. J. Warren and L. M. Meyer, *J. Solid State Chem.*, 1998, **138**, 178.
10 F. J. Morin, *Phys. Rev. Lett.*, 1959, **3**, 34.
11 B. S. Guition, Q. Gu, L. A. Prieto, M. S. Gudiksn and H. Park, *J. Am.Chem. Soc.*, 2005, **127**, 499.
12 E. Strelcov, Y. Lilach and A. Kolmakov, *Nano Lett.*, 2009, **9**, 2324.
13 S. Bonora, U. Bortolozzo, S. Residori, R. Balu and P. V. Ashrit, *Opt. Lett.*, 2010, **35**, 104.
14 H. T. Kim, B. G. Chae, D. H. Youn, S. L. Maeng, G. Kim, K. Y. Kang and Y. S. Lim, *New J. Phys.*, 2004, **6**, 52.
15 J. W. Hou, J. W. Zhang, Z. P. Wang, Z. M. Zhang and Z. J. Ding, *J.Nanosci. Nanotechnol.*, 2013, **13**, 1546.
16 F. Théobald, J. *Less-Common Met.*,1977, **53**, 55.
17 Y. Oka, S. Sato, T. Yao and N. Yamamoto, *J. Solid State Chem.*, 1998, **141**, 595.
18 M. Li, F. G. Kong, Y. X. Zhang, L. Chen, W. W. Yan and G. H. Li, *Dalton Trans.*, 2011, **40**, 10964.
19 S. D. Zhang, B. Shang, J. L. Yang, W. S. Yan, S. Q. Wei and Y. Xie, *Phys. Chem. Chem. Phys.*, 2011, **13**, 15880.
20 T. Yao, Y. Oka and N. Yamamoto, *J. Solid State Chem.*, 1994, **112**, 197.
21 J. Galy, *J. Solid State Chem.*, 1999, **148**, 226.
22 E. U. Donev, R. Lopez, L. C. Feldman and R. F. Haglund, *Nano Lett.*, 2009, **9**, 703.
23 S. X. Zhang, J. Y. Chou and L. J. Lauhon, *Nano Lett.*, 2009, **9**, 4528.
24 J. Mendialdua, R. Casanova and Y. Barbaux, *J. Electron Spectrosc. Relat. Phenom.*, 1995, **71**, 252.
25 C. X. Cao, Y. F. Gao and H. J. Luo, *J. Phys. Chem. C*, 2008, **112**, 11813.
26 Z. F. Peng, W. Jiang and H. Liu, *J. Phys. Chem. C*, 2007, **111**, 1121.
27 K. W. Lee, J. J. Kweon, C. E. Lee, A. Gedanken and R. Ganesan, *Appl. Phys. Lett.*, 2010, **96**, 243111.
28 J. M. Baik, M. H. Kim, C. Larson, A. M. Wodtke and M. Martin, *J. Phys. Chem. C*, 2008, **112**, 13330.
29 Y. F. Sun, S. S. Jiang, W. T. Bi, X. G. Tan, C. Z. Wu, S. Q. Wei and Y. Xie, *Nanoscale*, 2011, **3**, 4394.
30 J. C. Valmalette and J. R. Gavarri, *Mater. Sci. Eng. B*, 1999, **54**, 168.
31 I. L. Botto, M. B. Vassallo, E. J. Baran and G. Minelli, *Mater. Chem.Phys.* 1997, **50**, 269.
32 P. Schible, *Physica B*, 2002, **316**, 601.
33 S. Kim, K. Kim, C. J. Kang and B. I. Min, *Phys. Rev. B*, 2013, **87**, 195106.
34 J. M. Atkin, S. Berweger, E. K. Chavez and M. B. Raschke, *Phys.Rev. B*, 2012, **85**, 020101.